A new calibration to determine the closure temperatures of Fe-Mg ordering in augite from nakhlites

UNIVERSITÀ DEGLI STUDI DI TORINO

REVISED VERSION #2

A NEW CALIBRATION TO DETERMINE THE CLOSURE TEMPERATURES OF Fe-Mg ORDERING IN AUGITE FROM NAKHLITES

Alvaro M.[1*], Domeneghetti M.C.[2] , Fioretti A.M.[3], Cámara F.[4,5], Marinangeli L.[6]

[1]Dipartimento di Geoscienze, Università degli Studi di Padova, Italy
[2]Dipartimento di Scienze della Terra e dell'Ambiente, Università degli Studi di Pavia, Italy
[3]Istituto di Geoscienze e Georisorse CNR, UOS di Padova, Italy
[4]Dipartimento di Scienze della Terra, Università di Torino, Italy
[5] CrisDi, Interdepartmental Centre for the Research and Development of Crystallography, Torino, Italy
[6]Int'l Research School of Planetary Sciences, Università G. d'Annunzio, Chieti, Italy.

*Corresponding author e-mail: **matteo.alvaro@unipd.it**

For submission to: **Meteoritics & Planetary Science**

Article type: **Article**

Running Title: **Geothermometer for nakhlites**

ABSTRACT

Recently it has been shown that the relatively low closure temperature (T_c) of 500(100)°C calculated for augite from Miller Range nakhlite (MIL 03346,13) using the available geothermometers would correspond to a slow cooling rate inconsistent with the petrologic evidence for an origin from a fast cooled lava flow. Moreover, previous annealing experiments combined with HR-SC-XRD on an augite crystal from MIL 03346 clearly showed that at 600°C the Fe^{2+}-Mg degree of order remained unchanged, thus suggesting that the actual T_c is close to this temperature.

In order to clarify this discrepancy we undertook an *ex situ* annealing experimental study at 700, 800 and 900 °C, until the equilibrium in the intracrystalline Fe^{2+}-Mg exchange is reached, using an augite crystal from Miller Range nakhlite (MIL 03346,13) with composition ca. $En_{36}Fs_{24}Wo_{40}$. These data allowed us to calculate the following new geothermometer calibration for Martian nakhlites:

$$\ln k_D = -4421(\pm561)/T(\mathrm{K}) + 1.46(\pm0.52)\ (R^2=0.988),\ \text{where}\ k_D = [(Fe^{2+}_{M1})(Mg_{M2}) / (Fe^{2+}_{M2})(Mg_{M1})].$$

The application of this new equation to other Martian nakhlites (NWA 988 and Nakhla) suggests that for augite with composition close to that of MIL 03346, the T_c is up to 170°C higher with respect to the one calculated using the previous available geothermometer equation, thus suggesting a significantly faster cooling in agreement with petrologic evidence.

Keywords: augite, closure temperature, Martian nakhlite, single crystal X-ray diffraction, thermal history, geothermometer.

INTRODUCTION

The broadest application of intracrystalline Fe^{2+}-Mg partitioning between the *M*1 and *M*2 crystallographic sites in the pyroxene structure is the determination of the closure temperature (T_c) of the exchange reaction, that provides important constraints on the cooling rate of the pyroxene-bearing host rocks (e.g. Ganguly and Domeneghetti 1996). The partition coefficient, k_D, of the order-disorder Fe^{2+}-Mg reaction depends on the closure temperature of the exchange equilibrium, which in turn is affected by the sample cooling rate. Although this technique has been successfully developed (Virgo and Hafner 1969; Saxena and Ghose 1971; Smyth 1973; Sueno et al. 1976; Ganguly 1982; Molin and Zanazzi 1991; Sykes-Nord and Molin 1993; Ganguly and Domeneghetti 1996; Stimpfl et al. 1999; Pasqual et al. 2000; Alvaro et al. 2011) and applied for orthopyroxene and pigeonite-bearing rocks, relatively few data are available for clinopyroxenes (McCallister et al. 1976; Dal Negro et al. 1982; Ghose and Ganguly 1982; Molin and Zanazzi 1991 and Brizi et al. 2000). For clinopyroxenes, the extent of Fe-Mg exchange is limited, because the *M*2 site is mainly occupied by Ca and Na [Ca + Na ≈ 0.7–1.0 atoms per formula unit (apfu) in magmatic clinopyroxenes]. The most recent calibration for clinopyroxenes has been provided by Brizi et al. (2000). The geothermometer based on Fe^{2+}-Mg exchange in calcic clinopyroxenes has been tested in some Earth and planetary geological contexts (Malgarotto et al. 1993a,b; Abdu et al. 2009), providing T_c consistent with the other geological evidence. However, when applied to augites extracted from MIL 03346 and other nakhlites, this calibration yielded T_c for augite (Domeneghetti et al. 2013) that appears inconsistent with the fast cooling rates inferred from: (i) petrographic textures (Treiman, 2005); (ii) pyroxene morphologic characters (Hammer, 2006); (iii) olivine Fe-Mg and Ca zoning profiles and ilmenite exsolution (Mikouchi, et al. 2012) and (iv) experimental results on mineral equilibria (Herd and Walton, 2008). In order to account for these evident discrepancies Domeneghetti et al. (2013) suggested that either Brizi et al. (2000) calibration was, for some reason, unsuitable for the special composition of nakhlite clinopyroxenes or the augite geothermometer was disclosing some complexity in the nakhlites final cooling history. To further investigate this issue we undertook a new '*ex situ*' equilibrium annealing study combined with high-resolution single-crystal X-ray diffraction (HR-SC-XRD) experiments on augite crystals from Miller Range nakhlite (MIL 03346,13) with composition ca. $En_{36}Fs_{24}Wo_{40}$, in order to obtain a new thermometric calibration for nakhlites.

The reliability of our newly proposed geothermometer over a wide range of temperatures, has been evaluated through its application to the fast cooled terrestrial sample FON39 (Brizi et al. 2000),

a sample with composition close to that of MIL 03346. Furthermore these data have been compared with those reported by Domeneghetti et al. (2013) for sample Theo's flow, regarded as a terrestrial analogue for MIL 03346 (Lentz et al. 1999; 2011) in order to gain comparative information on the possible stratigraphic and geological setting for nakhlites. Finally, a tentative calculation of the cooling rates of these samples has been performed combining the newly collected data and the kinetic data from literature (e.g. Brizi et al. 2001 and Domeneghetti et al. 2013).

Formatted: Highlight

MATERIAL AND METHODS

Samples

Miller Range (MIL 03346,13), Northwest Africa (NWA 998) and Nakhla are augite-rich igneous rocks formed in flows or shallow intrusions of basaltic magma on Mars (see Treiman 2005). Samples MIL 03346, NWA 998 and Nakhla have been found in Miller Range, Antarctica, Northwest Africa and El Nakhla al Baharia, Egypt, respectively (Treiman 2005 and references therein).

All the augite samples from these rocks show homogeneous cores and iron-enriched rims (Treiman 2005). The core compositions are ca. $Wo_{40}En_{36}Fs_{24,}$ $Wo_{39}En_{38}Fs_{23}$, $Wo_{38}En_{38}Fs_{24}$, respectively for MIL 03346, NWA 998 and Nakhla. The terrestrial sample considered in this work, FON39, is a dacite lava flow from Fonualei Island (Tongan archipelago, S.E. Pacific Ocean) containing augite crystals with composition ca. $Wo_{37}En_{36}Fs_{27}$.

A small fragment (0.10 g) of MIL 03346,13 was obtained from the meteorite sample curator of NASA Johnson Space Center, whereas crystals from the NWA 998, FON39 and Nakhla samples have been kindly provided by A.J. Irving, G.M. Molin and the meteorite curator at the Natural History Museum of London, C. Smith, respectively.

A careful selection of pyroxene single crystals under the polarizing microscope was performed. Moreover, for MIL 03346, NWA 998 and Nakhla small core single crystals were obtained by cutting off the zoned rims and have been labelled MIL N.14 (see Domeneghetti et al. 2013) and N.19, NWA 998 N.11 and Nakhla N.1. One single crystal from FON39 (here labelled FON39 N.1) has been selected from the abovementioned batch of crystals used by Brizi et al. (2000). All the selected crystals showed sharp extinction and sharp diffraction profiles and were therefore considered to be suitable for X-ray data collection. Crystal MIL N.19 was selected for the annealing experiments.

Electron microprobe analysis

Crystals NWA 998 N.11 and Nakhla N.1 were embedded in epoxy resin and polished for electron microprobe analysis. A Cameca-SX50 electron microprobe with a fine-focused beam (1

μm diameter) operating in the wavelength-dispersive (WDS) mode was used. Operating conditions were 15 kV accelerating voltage and 15 nA beam current; counting times were 20 s at the peak and 20 s at the background. The following synthetic end-member mineral standards were used: diopside for Mg, ferrosilite for Fe, wollastonite for Si and Ca, chromite for Cr, corundum for Al, $MnTiO_3$ for Mn and Ti, and a natural albite (Amelia albite) for Na. X-ray counts were converted into oxide weight percentages using the PAP correction program. Analyses are precise to within 1% for major elements and 3-5% for minor elements. The results of the chemical analysis are reported in Table 1. The crystal chemical formula was calculated on the basis of six oxygen atoms,. Only those spot analyses with total cation contents of 4.000 ± 0.005 atoms on the basis of six oxygen atoms and charge balance $3^{[4]}Al + Na - 3^{[6]}Al - 4Ti - 3Cr - 3Fe^{3+} \leq |0.005|$ were selected and averaged. The Fe^{3+} content was calculated by stoichiometry following Droop (1987).

The values of 37.09(14), 36.64(10), 36.68(14) e.p.f.u. calculated from the analysis of crystal MIL N.1 (Domeneghetti et al. 2013), NWA 998 N.1, Nakhla N.1, respectively, are in very good agreement with the sum of the observed m.a.n.s for the *M*1 and *M*2 sites obtained from the structure refinement, before introducing chemical constraints, i.e. 37.07(6), 37.21(6), 36.66(6), 36.72(6) e.p.f.u. for crystals MIL N.14 and 19, NWA 998 N.11, Nakhla N.1, respectively (see Table 1 and Table 2).

Annealing experiment and X-ray diffraction

The annealing experiments have been carried out at 700, 800 and 900°C using MIL N.19 sample until the equilibrium in the Fe^{2+}-Mg exchange reaction was reached. The crystal was sealed into a silica vial, after alternate flushing with nitrogen and evacuating, together with an iron-wüstite buffer to control the oxygen fugacity fO_2. Inside the silica tube, the crystal and the buffer were put into two small separate Pt crucibles to avoid contact between them. After equilibrium in the Fe-Mg exchange reaction was reached quenching was performed by dropping the tubes into cold water. Further details on the annealing protocol used are given in Alvaro et al. (2011) and Domeneghetti et al. (2013).

HR-SC-XRD data (i.e. up to 0.434 $Å^{-1}$) were collected on crystal MIL N.19 before and after each annealing experiment using a three-circle Bruker AXS SMART APEX diffractometer, equipped with a CCD detector and 0.3mm MonoCap collimator (graphite-monochromatized Mo$K\alpha$ radiation, λ = 0.71073 Å operating 55 kV, 30 mA) following the same procedure described in Domeneghetti et al. (2013). The same data collection protocol has been adopted for crystals NWA 998 N.11, Nakhla N.1 and FON39 N.1. Data reduction has been performed for each sample following the procedure described in detail by Domeneghetti et al. (2013) for MIL 03346 crystals.

The samples' site distribution were obtained through full-matrix least-squares refinements carried out with SHELX program (Sheldrick 1997) as described in Domeneghetti et al. (2013). Chemical constraints have been taken from the microprobe analysis as reported in Table 1[1] for NWA 998 N.11 and Nakhla N.1 and those reported in literature for MIL03346, FON39 (Domeneghetti et al. 2013; Brizi et al. 2000, respectively), assuming 1σ as the error.

For all crystals the constraints reported in Domeneghetti et al. (2013) were also introduced into the refinement. For each crystal considered in this study the results obtained from the structural refinement (i.e. unit-cell parameters, discrepancy indices R_{all} and R_w based on all the F_o^2, the goodness of fit) are reported in Table 2. The site populations obtained from the structural refinements with chemical constraints are reported in Table 3.

RESULTS AND DISCUSSION

Determination of the Fe^{2+}-Mg ordering state

The Fe^{2+}-Mg ordering state was estimated from the site population (Table 3) by means of the intracrystalline distribution coefficient k_D, using the same expression adopted by Brizi et al. (2000): $k_D = [(Fe^{2+}_{M1})(Mg_{M2})/(Fe^{2+}_{M2})(Mg_{M1})]$. The k_D values and relative propagated errors obtained are reported in Table 3.

An attempt at structural refinement was also performed by considering Mn fully ordered in the M2 site in agreement with the stronger preference for the M2 site of Mn compared to Fe^{2+}, observed by Stimpfl (2005a, 2005b) in a donpeacorite sample. Because of the low Mn contents of the selected samples (see Domeneghetti et al. 2013 and Brizi et al. 2000) this procedure did not significantly affect the k_D values.

Formatted: (Asian) Japanese, Highlight

New geothermometer and evaluation of the closure temperatures for augite samples

For the two MIL 03346 crystals k_D ranges from 0.026(5) to 0.028(5), in very good agreement with those found for the other two nakhlite samples of 0.027(5) and 0.025(4) for NWA 998 N.11 and Nakhla N.1, respectively, confirming the very similar rock history and evolution of these samples. The k_D value obtained on crystal FON39 N.1 [k_D = 0.080(5)] is identical within estimated standard deviations (e.s.d.'s) to that reported by Brizi et al. (2000).

In Fig. 1 $\ln k_D$ is plotted against $1/T$ for MIL 03346 crystal N.19 (this study), N.14 from Domeneghetti et al. (2013), together with the literature data from Brizi et al. (2000). Weighted linear regression of $\ln k_D$ versus $1/T$ for the four temperatures (600, 700, 800 and 900°C) at which crystals MIL N.14 and N.19 were annealed yields the following equation:

[1] **Table 2** has been deposited as supplementary material.

$$\ln(k_D = -4421(\pm 561)/T(K) + 1.46(\pm 0.52)(R^2 = 0.988)$$

where $k_D = [(Fe^{2+}_{M1})(Mg_{M2})/(Fe^{2+}_{M2})(Mg_{M1})]$.

The closure temperature obtained for MIL 03346 N.14 and N.19, NWA 998 N.11, Nakhla N.1 and FON39 N.1 with this new geothermometer are reported in Table 3, together with those obtained using the calibration by Brizi et al. (2000) on a crystal from sample FON39. As already expected from their comparable k_D values, the T_c calculated for the three nakhlites are identical within estimated standard deviation, ranging from 585(83)°C for Nakhla N.1 to 594(87)°C for MIL N. 14. The precision of our method does not permit to reliably assess if there is a significant difference between the closure temperatures of Fe-Mg ordering in clinopyroxenes in MIL 03346 and NWA 998 samples, unlike as indicated by petrological and textural evidence (see Treiman 2005; Hammer 2009, Mikouchi et al. 2012).

At the same time this study shows that the geothermometer calibrated by Brizi et al. (2000) underestimates the nakhlites pyroxene T_c by ca. 170°C (see Table 3 and Fig. 1). In particular, the T_c calculated using the equation obtained by Brizi et al. (2000) for crystal FON39 N.1 (which has a composition close to that of the nakhlite pyroxenes investigated in this study) leads to the discrepancies up to about 170°C (i.e. far beyond their e.s.d.'s). The $\ln k_D$ vs. 1/T relation for sample FON39 N.1-, as determined in this study, is illustrated in Fig. 1 and compared with that of Brizi et al. (2000). A possible explanation for the large disagreement between the two calibrations is that there was a large error in the determination of the furnace temperature in the experiments of Brizi et al. (2000). However, the T_c calculated for FON39 N.1 using our geothermometer (T_c = 836°C) is still well below their first recalculated annealing T, being 922°C instead of the published 750°C. Therefore, such a temperature difference would explain why the crystal was actually disordering. Moreover, our T_c of 836°C seems to be reasonable considering the presence of volcanic glass in the groundmass of FON39 dacite host rock .

Formatted: (Asian) Japanese, Highlight

Further evidence of the mismatch is provided by the calculation of the closure temperature for other augite samples with different X_{Fe} and degree of order available in the literature regardless of the clinopyroxene composition, i.e. Theo's flow clinopyroxene (TS7 by Domeneghetti et al. 2013), KC (andesitic dike) and PD30 (basaltic dike) by Brizi et al. (2000). In fact, the T_c calculated with our new geothermometer for Theo's flow clinopyroxene (ca. 700°C, with k_D ca. 0.05), KC and PD30 (ca. 900°C, k_D ca. 0.1) are about 100, 89 and 52 °C higher, respectively, than those obtained using the equation by Brizi et al. (2000).

In order to evaluate the effect of such differences in closure temperature on the thermal history of these samples a reliable Arrhenian relation for augite is needed. However, the only available kinetic data for clinopyroxenes are those published by (i) Brizi et al. (2001) for an augite

sample with composition $Wo_{43}En_{46}Fs_{11}$ and (ii) Domeneghetti et al. (2005) for a $P2_1/c$ pigeonite sample with composition $Wo_{10}En_{47}Fs_{43}$. Therefore, bearing in mind that these Arrhenian relations are not suitable for our Martian sample composition, a tentative calculation of the cooling rates for all samples has been done. Because of the abovementioned discrepancies between our equilibrium data and those by Brizi et al. (2000) we decided to calculate the cooling rate using both the kinetic data of Brizi et al. (2001) and those by Domeneghetti et al. (2005) after correcting for the different Ca content. The cooling rate have been modelled using an asymptotic cooling law: $1/T(\mathrm{K}) = 1/To + \eta t$ (where η is the cooling time constant, Ganguly 1982) and assuming fO2 conditions for Martian samples equal to that of IW +2.65 (Domeneghetti et al., 2013). The calculation was carried out using the program CRATE (Ganguly pers. comm.). The $C_{0(\mathrm{augite})}$ for each sample has been obtained through a correction factor, that accounts for their Ca content, starting from $C_{0(\mathrm{pigeonite})}$ following the procedure reported in Ganguly (1982) for diopside from Lesotho Kimberlite pipe. The resulting cooling rates calculated using Brizi et al. (2001) Arrhenian relation at their respective T_c are 6.8, 4.2, 2.7, 4.8 and 51.3°C/h for MIL 03346, NWA 998, Nakhla, Theo's Flow and Fon39, respectively. On the other hand, the cooling rates calculated at their respective T_c using the Arrhenian relation from Domeneghetti et al. (2005) corrected for the different Ca contents resulted in cooling rates one order of magnitude slower, being 0.16, 0.13, 0.13, 0.09 and 3°C/h for MIL 03346, NWA 998, Nakhla, Theo's Flow and Fon39, respectively. However, the slower cooling rate obtained on TS7 compared to that of nakhlites, despite its higher T_c (720°C for TS7 vs. ca. 600°C for the nakhlites), could be due to the differences in composition (i.e. Fe and Ca contents) that affect both equilibrium and kinetic behavior.

Cooling rates alone cannot be used to calculate the precise depths at which MIL 03346, NWA 998, Nakhla were cooling to around their respective T_c, because this calculation heavily depends on the choice of boundary conditions (Sears et al., 1997; Nabelek et al., 2002; Vorsteen and Schellschmidt, 2003) which are still fairly unconstrained for nakhlites. However, as a tentative exercise, assuming a T_0=1150 °C for the nakhlite magma (Stockstill et al. 2005); $T_{air} = T_{bedrock} = 0$ °C at the time of magma extrusion (Treiman, 2003; Shuster and Weiss, 2005), a thermal diffusivity of 31.5 m^2/y, and using the simplified mathematical model for cooling of volcanic bodies proposed by Jaeger (1968), we obtained a burial depth in the range 2.5 - 2.7 m for the three nakhlite samples, at the T_c and cooling rates calculated with the new calibration. The pyroxene closure temperatures of the three nakhlites and their cooling rates at the T_c are identical within error and therefore it would be meaningless to try to distinguish the individual burial depths. As a further exercise we calculated the burial depth of Theo's flow sample TS7 and compared the resulting burial depth with the actual position of the sample within the lava sequence, as observed in the field.

Formatted: Highlight

Assuming a single magma unit of 120 m erupted at T_0=1140 °C (Lentz et al., 2011), we could not find any solution for a cooling rate of = 0.091 °C/h at a T_c = 720 °C . We observe, however, that these cooling conditions are fulfilled in a lava flow of ca. 50 m (the same thickness as the pyroxenite layer), at a burial depth of ca. 40 m, which is close to the position of this sample within the pyroxenite layer. This appears to suggest that Theo's flow is not a single 120m magma unit, but possibly represents multiple injections. It is worth noting that using the cooling rate values obtained with Brizi et al. (2001) calibration, the same exercise cannot provide a realistic solution for the burial depth of pyroxene in either the nakhlites or Theos' flow.

CONCLUSIONS

Our new calibration of the Fe-Mg exchange geothermometer, experimentally obtained on augite from the nakhlite MIL 03346, provides a significant revision of the Brizi et al. (2000) augite geothermometer. The new calibration yields closure temperatures (T_c) of the augite Fe-Mg exchange significantly higher than those calculated with the previous calibration.

Tentative calculation of the cooling rates of the host lava, at the Tc of augite, allow evaluation of burial depths and yield values of 2-3 m for the three nakhlite samples. Closure temperatures and cooling rates for the three nakhlites, which are identical within errors, do not permit any meaningful comparison between their burial depths.

However, these calculated cooling rates allow reconciliation of the relatively low augite T_c obtained from MIL 03346 (and other nakhlites), with the petrographic and textural evidence for a fast cooling. Moreover, it is clear that the nakhlites T_c (about 600°C) is lower than that calculated for TS7 (720 °C) sample, which was supposed to be cooled within Theo's lava flow at a burial depth of 85 m.

Acknowledgments

The authors wish to thank J. Ganguly and M. Tribaudino for their helpful suggestions and improvements. We thank Allan Treiman for kindly supplying Theo's flow sample. M.C Domeneghetti was supported by the Italian PNRA PEA2013/Meteoriti Antartiche to L. Folco, A.M. Fioretti by the *Programma Nazionale Ricerche in Antartide* (PNRA), L. Marinangeli and M. Alvaro by the Italian Space Agency grant (n. I/060/10/0) for the MARS-XRD/ExoMars project. M. Alvaro has been also supported by the ERC starting grant #307322 to F. Nestola. R. Gastoni (C.N.R. – IGG Pavia) is thanked for sample preparation and R. Carampin (C.N.R. – IGG Padova) is thanked for helping with EMPA analyses. Authors are grateful to M. Faccenda for fruitful discussion on modeling of burial depth.

REFERENCES

Abdu Y. A., Scorzelli R. B., Varela M. E., Kurat G., Azevedo I. d. S., Stewart S. J., and Hawthorne F. C. 2009. Druse clinopyroxene in D'Orbigny angritic meteorite studied by single-crystal X-ray diffraction, electron microprobe analysis, and Mössbauer spectroscopy. *Meteoritics & Planetary Science* 44: 581-587.

Alvaro M., Cámara F., Domeneghetti M., Nestola F., and Tazzoli V. 2011. H*T* $P2_1/c$–*C*2/*c* phase transition and kinetics of Fe^{2+}–Mg order–disorder of an Fe-poor pigeonite: implications for the cooling history of ureilites. *Contributions to Mineralogy and Petrology* 162: 599-613.

Brizi E., Molin G., and Zanazzi P. F. 2000. Experimental study of intracrystalline Fe^{2+}-Mg exchange in three augite crystals: Effect of composition on geothermometric calibration. *American Mineralogist* 85: 1375-1382.

Dal Negro A., Carbonin S., Molin G., Cundari A., and Piccirillo E. 1982. Intracrystalline cation distribution in natural clinopyroxenes of tholeiitic, transitional, and alkaline basaltic rocks. In *Advances in Physical Geochemistry*, pp. 117-150. Springer.

Domeneghetti M., Fioretti A., Cámara F., McCammon C., and Alvaro M. 2013. Thermal history of nakhlites: A comparison between MIL 03346 and its terrestrial analogue Theo's flow. *Geochimica et Cosmochimica Acta* 121: 571-581.

Droop G. T. R. 1987. A general equation for estimating Fe^{3+} concentrations in ferromagnesian silicates and oxides from microprobe analyses, using stoichiometric criteria. *Mineralogical Magazine* 51: 431-435.

Ganguly J. (1982) Mg-Fe order-disorder in ferromagnesian silicates: II. Thermodynamics, kinetics and geological applications. Advances in Physical Geochemistry 2:58-99

Ganguly J. and Domeneghetti M. C. 1996. Cation ordering of orthopyroxenes from the Skaergaard Intrusion: implications for the subsolidus cooling rates and permeabilities. *Contributions to Mineralogy and Petrology* 122: 359-367.

Formatted: Highlight

Ghose S. and Ganguly J. 1982. Mg-Fe order-disorder in Ferromagnesian silicates. In *Advances in Physical Geochemistry* (ed. S. Saxena), pp. 3-99. Springer New York.

Hammer J. E. 2006. Influence of fO_2 and cooling rate on the kinetics and energetics of Fe-rich basalt crystallization. *Earth and Planetary Science Letters* 248: 618-637.

Hammer J. E. 2009. Application of a textural geospeedometer to the late-stage magmatic history of MIL 03346. *Meteoritics & Planetary Science* 44: 141-154.

Herd C. and Walton E. 2008. Cooling and crystallization of the Miller Range 03346 nakhlite: Insights from experimental petrology and mineral equilibria. In *Lunar and Planetary Institute Science Conference Abstracts*, pp. 1496.

Jaeger, J.C. 1968. Cooling and solidification of igneous rocks. In Hess, H.H. & Poldervaart, A. , "Basalts". Vol. 2, Interscience. Publ., New York, 503- 536.

Lentz R. C. F., Taylor G. J., and Treiman A. H. 1999. Formation of a martian pyroxenite: A comparative study of the nakhlite meteorites and Theo's Flow. *Meteoritics & Planetary Science* 34: 919-932.

Lentz R. C. F., McCoy T. J., Collins L. E., Corrigan C. M., Benedix G. K., Taylor G. J., and Harvey R. P. 2011. Theo's Flow, Ontario, Canada: A terrestrial analog for the Martian nakhlite meteorites. *Geological Society of America Special Papers* 483: 263-277.

Malgarotto C., Molin G., and Zanazzi P. F. 1993a. Cooling history of a dyke on Alicudi (Aeolian Islands) from intracrystalline Fe^{2+} -Mg exchange reaction in clinopyroxene. *European Journal of Mineralogy* 5: 755-762.

Malgarotto C., Molin G., and Zanazzi P. F. 1993b. Crystal chemistry of clinopyroxenes from Filicudi and Salina (Aeolian Islands, Italy); geothermometry and barometry. *European Journal of Mineralogy* 5: 915-923.

McCallister R. H., Finger L. W., and Ohashi Y. 1976. Intracrystalline Fe (super 2+) -Mg equilibria in three natural Ca-rich clinopyroxenes. *American Mineralogist* 61: 671-676.

Mikouchi T., Makishima J., Kurihara T., Hoffmann V. H. and Miyamoto M. 2012. Relative burial depth of nakhlites revisited. 43rd Lunar and Planetary Science Conference. Abstract #2363.

Molin G. and Zanazzi P. F. 1991. Intracrystalline Fe^{2+}-Mg ordering in augite: experimental study and geothermometric applications. *European Journal of Mineralogy* 3: 863-875.

Nabelek P.I., Hofmeister A.M., Whittington A.G. 2002. The influence of temperature-dependent thermal diffusivity on the conductive cooling rates of plutons and temperature-time paths in contact aureoles. Earth and Planetary Science Letters, 317–318; 157–164.

Pasqual D., Molin G., and Tribaudino M. 2000. Single-crystal thermometric calibration of Fe-Mg order-disorder in pigeonites. *American Mineralogist* 85: 953-962.

Saxena S. K. and Ghose S. 1971. Mg^{2+}-Fe^{2+} order-disorder and the thermodynamics of the orthopyroxene crystalline solution. *American Mineralogist* 56: 532-559.

Sears D.W.G., Symes S.J.K., Batchelor J.D., Akridhe D.G., and Benoit P.H. 1997. The metamorphic history of eucrites and eucrite-related meteorites and the case for late metamorphism. Meteoritics & Planetary Science 32: 917-927.

Sheldrick G. M. 1997. SHELXL-97, program for crystal structure refinement. *University of Göttingen, Germany*: 97-2.

Shuster D.L, and Weiss B.P. 2005. Martian Surface Temperature from Thermochronology of Meteorites. Science Vol. 309 no. 5734 pp. 594-600 DOI: 10.1126/science.1113077.

Smyth J. 1973. Orthopyroxene structure up to 850°C. *American Mineralogist* 58: 636-648.

Formatted: Highlight

Stimpfl M., Ganguly J., and Molin G. 1999. Fe2+-Mg order-disorder in orthopyroxene: equilibrium fractionation between the octahedral sites and thermodynamic analysis. *Contributions to Mineralogy and Petrology* 136: 297-309.

Stockstill K. R., McSween H. Y., Jr., and Bodnar R. J. 2005. Melt inclusions in augite of the Nakhla Martian meteorite: Evidence for basaltic parental melt. Meteoritics & Planetary Science 40: 377–398.

Sueno S., Cameron M., and Prewitt C. 1976. Orthoferrosilite: high-temperature crystal chemistry. *American Mineralogist* 61: 38-53.

Sykes-Nord J. A. and Molin G. 1993. Mg-Fe order-disorder reaction in Fe-rich orthopyroxene; structural variations and kinetics. *American Mineralogist* 78: 921-931.

Treiman A.H. 2003. Submicron magnetite grains and carbon compounds in Martian meteorite ALH84001: inorganic, abiotic formation by shock and thermal metamorphism. Astrobiology 3(2): 369–392.

Treiman A. H. 2005. The nakhlite meteorites: Augite-rich igneous rocks from Mars. *Chemie der Erde - Geochemistry* 65: 203-270.

Virgo D. and Hafner S. 1969. Fe^{2+}, Mg order-disorder in heated orthopyroxenes. *Pyroxenes and amphiboles: crystal chemistry and phase petrology*: 67.

Vosteen H-D. and Schellschmidt R. 2003. Influence of temperature on thermal conductivity, thermal capacity and thermal diffusivity for different types of rock. Physics and Chemistry of the Earth 28: 499-509.

Figures and Tables

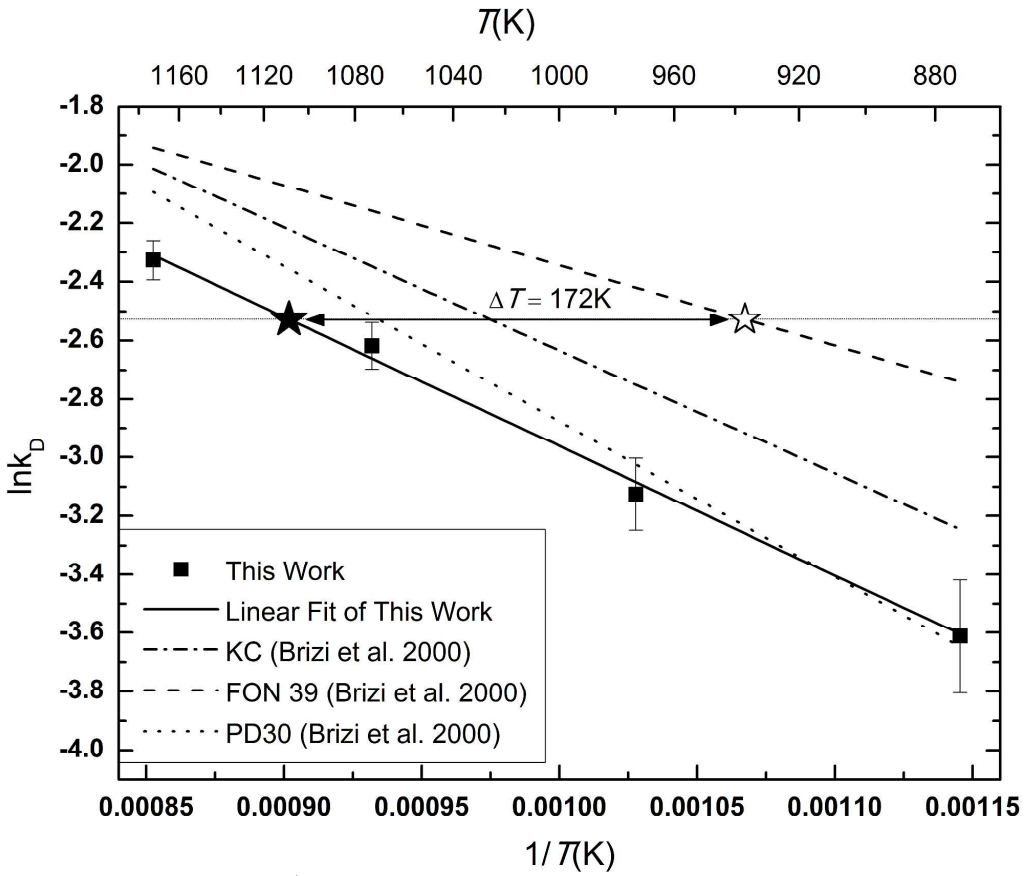

Fig. 1. Lnk_D versus $1/T$ (K^{-1}) for the augite samples considered in this work together with those reported by Brizi et al. (2000) for FON39, PD30 and KC samples. Solid line represents geothermometer equation calibrated by linear fitting of MIL N.19 data. Filled star and open star represent the closure temperature calculated for FON39 N.1 with our geothermometer calibration and with that of Brizi et al. (2000), respectively.

Table 1. Electron microprobe analyses and formulae in atoms per formula unit (apfu) based on six oxygen atoms.

	Cpx Nakhla N.1 (averaged spots (44)	Cpx NWA 998 N.11 (averaged spots 8)
	% oxides	
SiO_2	52.30 (22)	51.14(18)
TiO_2	0.11(3)	0.34(2)
Al_2O_3	0.45 (2)	1.02(3)
Cr_2O_3	0.43(5)	0.44(3)
FeO	14.33 (23)	13.40(31)
Fe_2O_3	-	-
MnO	0.45(4)	0.42(4)
MgO	13.39(15)	12.99(15)
CaO	18.35(13)	18.84(14)
Na_2O	0.14(4)	0.27(4)
K_2O	0.01(1)	0.00
Total	97.97(41)	99.06(13)
	a.p.f.u.	
Si	1.983(6)	1.953(4)
Ti	0.003(1)	0.010 (1)
Al	0.020(1)	0.046(2)
Cr	0.013(1)	0.013(1)
Fe^{2+}	0.448(6)	0.401(9)
Fe^{3+}	0.006(6)	0.033(5)
Mn	0.014(1)	0.014(1)
Mg	0.757(8)	0.740(8)
Ca	0.745(5)	0.771(5)
Na	0.011(3)	0.020(3)
K	0.000(1)	0.000(2)
Total	4.000(2)	4.001(2)
m.a.n.*	36.68(14)	36.68(17)

m.a.n.*: calculated total mean atomic number for M1 and M2 sites, in electrons per formula unit (a.p.f.u).

Table 2. Unit cell parameters and information on data collection and structure refinement for untreated NWA 998 N.11, Nakhla N.1 MIL N.19 and FON39 N.1. Data for MIL N.19 obtained after each annealing temperature (700, 800 and 900°C) are also reported.

	NWA 998 N.11	Nakhla N.1	MIL N.19				FON39 N.1
	Untreated	Untreated	Untreated	700°C	800°C	900°C	Untreated
Crystal sizes (mm)	0.170 x 0.128 x 0.050	0.185 x 0.185 x 0.090	0.170 × 0.120 × 0.080				0.100 x 0.087 x 0.060
a, *b*, *c* (Å)	9.7468(4), 8.9397(4), 5.2509(2)	9.7539(9), 8.9542(8), 5.2536(5)	9.7589 (5), 8.9484 (4), 5.2537 (2)	9.7559 (5), 8.9505 (4), 5.2538 (2)	9.7575 (4), 8.9507 (4), 5.2551 (2)	9.7603 (5), 8.9501 (4), 5.2553 (2)	9.7474 (4), 8.9385 (4), 5.2536 (2)
β (°)	106.2677(13)	106.382(3)	106.2246(17)	106.1946(17)	106.2057(15)	106.2451(18)	106.4000(18)
V (Å^3)	439.21(3)	440.21(7)	440.52(3)	440.56(3)	440.73(3)	440.75(3)	439.11(3)
μ (mm^{-1})	1.14	1.13	1.13	1.13	1.13	1.13	1.14
I_{ind}	2735	2724	2777	2785	2778	2785	2766
R_{int}	0.016	0.017	0.022	0.024	0.024	0.024	0.03
R_{all}, Rw, S	0.031, 0.080, 1.21	0.023,0.058, 1.14	0.028, 0.073, 1.06	0.029, 0.076, 1.04	0.027, 0.073, 1.06	0.029, 0.071, 1.07	0.034, 0.100, 1.15
m.a.n.[(a)]	36.66(6)	36.72(6)	37.21(6)	37.20(6)	37.13(6)	37.17(6)	36.73(6)

Standard deviations are given in parentheses. I_{ind} is the number of independent reflections used for structure refinement; $R_{int} = \Sigma \left| F_o^2 - F_o^2(\text{mean}) \right| / \Sigma [F_o^2]$ where F_o and F_c are the observed and calculated structure factors; $R_{all} = \Sigma \left| \left| F_o^2 \right| - \left| F_c^2 \right| \right| / \Sigma [F_o^2]$; $R_w = \{\Sigma [w(F_o^2 - F_c^2)^2] / \Sigma [w(F_o^2)^2]\}^{1/2}$; $S = [\Sigma [w(F_o^2 - F_c^2)^2]/(n-p)]^{0.5}$, where n is the number of reflections and p is the total number of parameters refined. [(a)] m.a.n. is the mean atomic number (in electrons per formula unit) before introducing the chemical constraints. Crystal system monoclinic *C*2/*c*; radiation type Mo*K*α.

Table 3. Site populations and k_D for Martian nakhlites obtained in this work (NWA 998 N.11 , Nakhla N.1, MIL N.19 and FON39 N.1) together with those reported by Domeneghetti et al. (2013) for sample MIL N.14

		NWA 998 N.11	NAKHLA N.1	MIL N.14		MIL N.19				FON39 N.1[(a)]
		Untreated	Untreated	Untreated	600° C	Untreated	700° C	800° C	900° C	Untreated
T	**Si**	1.954	1.983	1.964	1.965	1.964	1.965	1.965	1.964	1.976
	Al	0.047	0.017	0.036	0.035	0.036	0.036	0.035	0.036	0.024
M1	**Mg**	0.721(2)	0.732(2)	0.688(3)	0.689 (2)	0.688(2)	0.680 (2)	0.670 (2)	0.660 (2)	0.703(2)
	Fe	0.214(3)	0.229(3)	0.256(4)	0.257 (3)	0.257(3)	0.265 (3)	0.275 (3)	0.285 (3)	0.269(2)
	Fe^{3+}	0.035	0.013	0.026	0.021	0.028	0.029	0.027	0.027	0
	Al	0	0.003	0.007	0.01	0.004	0.003	0.004	0.004	0.012
	Cr	0.013	0.013	0.007	0.007	0.007	0.007	0.007	0.007	0.002
	Ti	0.01	0.003	0.008	0.008	0.008	0.008	0.008	0.008	0.005
	Mn	0.007	0.007	0.008	0.008	0.008	0.008	0.009	0.009	0.009
M2	**Mg**	0.018(3)	0.018(3)	0.015(3)	0.016 (3)	0.014(3)	0.021 (3)	0.032 (3)	0.039 (3)	0.047(3)
	Fe	0.196(2)	0.224(2)	0.191(4)	0.190 (4)	0.196(3)	0.188 (3)	0.178 (3)	0.170 (3)	0.223(3)
	Ca	0.758	0.733	0.768	0.769	0.765	0.767	0.766	0.767	0.722
	Mn	0.006	0.008	0.006	0.006	0.006	0.006	0.005	0.005	0.008
	Na	0.022	0.017	0.02	0.02	0.02	0.019	0.02	0.019	0
	k_D	0.027	0.025	0.028	0.031	0.026	0.043	0.073	0.098	0.080
	σk_D	0.005	0.005	0.005	0.005	0.005	0.005	0.006	0.007	0.005
	T_c (°C)[(b)]	411	397	405	416	434	497	636	734	664
	T_c (°C)[(c)]	601	585	594	605	623	684	811	895	836
	σT_c	87	83	87	84	83	67	43	31	33

Note: $k_D = [(Fe^{2+}_{M1})(Mg_{M2})/(Fe^{2+}_{M2})(Mg_{M1})]$, $R^{3+}=Fe^{3+} + Al + Cr + Ti$. The site occupancy values represent atoms per six oxygen atoms. (a) Chemical constraints introduced are based on the chemical analysis provided by Brizi et al. 2000). Closure temperature calculated using the geothermometer reported by Brizi et al. (2000) using a crystal from sample FON39 (b) and calculated using equation from this study (c). Standard deviations on closure temperatures have been calculated accounting for the linear regression errors.